UNCLASSIFIED

NRL Report 7641

# Electronic Surface Studies of Vacuum-Integrated-Circuit Components

HENRY F. GRAY AND GEORGE A. HAAS

*Electron Physics Branch*
*Electronics Division*

December 21, 1973

**NAVAL RESEARCH LABORATORY**
**Washington, D.C.**

Approved for public release; distribution unlimited.

UNCLASSIFIED

SECURITY CLASSIFICATION OF THIS PAGE *(When Data Entered)*

| REPORT DOCUMENTATION PAGE | | READ INSTRUCTIONS BEFORE COMPLETING FORM |
|---|---|---|
| 1. REPORT NUMBER<br>NRL Report 7641 | 2. GOVT ACCESSION NO. | 3. RECIPIENT'S CATALOG NUMBER |
| 4. TITLE *(and Subtitle)*<br>ELECTRONIC SURFACE STUDIES OF VACUUM-INTEGRATED-CIRCUIT COMPONENTS | | 5. TYPE OF REPORT & PERIOD COVERED<br>Final report on one phase of a continuing NRL problem.<br>6. PERFORMING ORG. REPORT NUMBER |
| 7. AUTHOR*(s)*<br>Henry F. Gray and George A. Haas | | 8. CONTRACT OR GRANT NUMBER*(s)* |
| 9. PERFORMING ORGANIZATION NAME AND ADDRESS<br>Naval Research Laboratory<br>Washington, D. C. 20375 | | 10. PROGRAM ELEMENT, PROJECT, TASK AREA & WORK UNIT NUMBERS<br>NRL Problem R08-58<br>A360360G/058B/3F53.533.602 |
| 11. CONTROLLING OFFICE NAME AND ADDRESS<br>Department of the Navy<br>Naval Air Systems Command<br>Washington, D. C. 20361 | | 12. REPORT DATE<br>December 21, 1973<br>13. NUMBER OF PAGES<br>16 |
| 14. MONITORING AGENCY NAME & ADDRESS*(if different from Controlling Office)* | | 15. SECURITY CLASS. *(of this report)*<br>Unclassified<br>15a. DECLASSIFICATION/DOWNGRADING SCHEDULE |
| 16. DISTRIBUTION STATEMENT *(of this Report)*<br>Approved for public release; distribution unlimited. | | |
| 17. DISTRIBUTION STATEMENT *(of the abstract entered in Block 20, if different from Report)* | | |
| 18. SUPPLEMENTARY NOTES | | |
| 19. KEY WORDS *(Continue on reverse side if necessary and identify by block number)*<br>Vacuum integrated circuits<br>Thermionic emission<br>Cathodes<br>Auger spectroscopy<br>Surface-potential mapping<br>Work function | | |

20. ABSTRACT *(Continue on reverse side if necessary and identify by block number)*

Microelectronic vacuum-integrated-circuit components have been studied to determine the emission capability of a newly developed electron emitter which is necessary for vacuum-integrated-circuit operation, to determine the surface-potential variations in the cathode and grid structures, and to determine the effects of migration, transport, and diffusion. The emission performance of the electron emitter, which can be delineated into small areas of almost any desirable shape by standard

(Continues)

DD FORM 1 JAN 73 1473 EDITION OF 1 NOV 65 IS OBSOLETE
S/N 0102-014-6601



SECURITY CLASSIFICATION OF THIS PAGE *(When Data Entered)*

20.

photolithographic processes, has been found to be comparable to standard sprayed oxide-coated cathodes, i.e., the effective work function $\phi_E(1000\ K) \approx 1.66 \pm 0.50$ eV and $\Delta\phi_E/\Delta T \approx 6.3 \times 10^{-4}$ eV/K. Using a scanning low-energy electron probe (SLEEP) and an Auger spectrometer, variations in surface potential on electron emitters and electrodes were correlated with chemical-element variations. Also, decreased resistance between electrodes after cathode activation was correlated with the presence of deposited barium and carbon components.

UNCLASSIFIED

## CONTENTS

INTRODUCTION ..... 1

ELECTRON EMISSION PROPERTIES OF KTFR OXIDE-COATED CATHODES ..... 1

MEASUREMENTS USING THE SCANNING LOW-ENERGY ELECTRON PROBE AND AN AUGER SPECTROMETER . 4

CONCLUSIONS ..... 12

REFERENCES ..... 12

UNCLASSIFIED

# ELECTRONIC SURFACE STUDIES OF VACUUM-INTEGRATED-CIRCUIT COMPONENTS

## INTRODUCTION

Electronic devices are needed that can withstand severe military environments such as high temperature and mechanical shock as well as nuclear radiation which might be encountered during guided-missile reentry into the atmosphere. Standard vacuum tubes, which are more radiation resistant then any known semiconductor, are bulky, have large power requirements, and together with their associated circuitry cannot tolerate some of the mechanical shock and high-temperature ambient conditions (e.g., 650 C). Semiconductor devices (e.g., ICs), though avoiding the size and power requirements of standard vacuum tubes, also cannot operate at the elevated temperatures required. A new technology which shows promise is the vacuum-integrated-circuit (1, 2). In addition to exhibiting the radiation resistance of vacuum tubes, vacuum-integrated-circuits can operate in high-temperature environments. They offer the advantages of high density, light weight, and ruggedness at a potentially low cost.

In this technology the approach is to design and develop microelectronic devices by the use of "vacuum-tube" electrodes deposited on a microelectronic chip. The chip is heated to approximately 600°C such that the cathode electrode emits electrons. The electrons are controlled by a coplanar grid electrode which is followed by one or more anode electrodes. Many of these miniature "vacuum tubes" would be deposited onto and interconnected on the same sapphire chip to provide the desired circuit function.

Though these devices show great potential, many questions must be answered prior to device development. Some of these questions concern the determination of: (a) the actual emission properties of the photolithographically delineated emissive material, Kodak Thin-Film Resist (KTFR) oxide-coated cathode (b) the surface-potential variations in the cathode and grid structures, and (c) migration and transport of emissive materials, diffusion of electrode metallization, and the poisoning effects, which occur at the high operating temperatures of these devices. All the previous factors determine how active components (e.g., diodes, triodes, pentodes) will have to be designed. This report describes some initial work on the electron-emission capabilities of KTFR cathodes as well as surface studies carried out on a pentode component by means of the Scanning Low-Energy Electron Probe (SLEEP) and an Auger spectrometer.

## ELECTRON-EMISSION PROPERTIES OF KTFR OXIDE-COATED CATHODES

Oxide-coated cathodes made from alkaline earth oxide mixtures have been used for many years as sources of electrons in vacuum (3 - 5). The usual method of applying such emissive coatings is by spraying, although other methods such as cataphoresis, dragging, and applications of sheets of binder and alkaline earth mixtures have also been used.

These methods, however, generally produce coatings which are rather fragile and cannot easily be delineated into very small emitting areas of arbitrary size and shape. By replacing the standard methylamylacetate nitrocellulose binder solution with KTFR, one can use normal photolithographic techniques to delineate emission areas to almost any planar size and shape (1, 2). However, realizing that oxide-coated cathodes are known to be sensitive to minute amounts of impurities and to excessively large amounts of carbon, the emission properties of KTFR oxide-coated emitters were studied.

The KTFR oxide-coated emitters* were prepared by depositing a solution of approximately 70% by weight of triple carbonate powder† and 30% KTFR negative photoresist binder onto an RCA N109 3-mm-diameter planar nickel emitter structure which was heated indirectly. After spinning the structure at 5000 rpm to remove excess photoresist binder mixture, the resultant emissive layer was approximately 25 $\mu$m thick. The emitter structures were then exposed to normal white light to polymerize the binder. They remained at atmospheric pressure until tested.

The emitters were studied in a 75-l/s Vacion/Vacsorb pumped UHV chamber designed specifically for electron-emitter studies. The chamber housed a copper anode cooled by turbulent-fast-flow water, a movable molybdenum shutter to prevent conversion products from contaminating the anode, and a planar guard assembly to minimize edge effects. Pt/Pt-10% Rh thermocouples 75 $\mu$m in diameter were attached to the edge of the emitter surfaces for temperature measurements. After baking at 300 C for 8 hr, the base pressure was in the $10^{-10}$ torr range. Emitter conversion was accomplished by heating the emitter slowly such that the pressure was kept below $4 \times 10^{-6}$ torr. Activation took place by heating to 1000 - 1065 C for about 2 min and then drawing space-charge-limited emission of approximately 0.1 A/cm$^2$ for 30 min at 910 C ($P \approx 10^{-9}$ torr).

For a determination of the work function from emission measurements, an accurate knowledge of the emitter temperature is essential, and it is common practice to use optical or infrared pyrometers for this measurement. Since these pyrometer measurements must be corrected for the spectral emissivity of the emitting surface, a Pt/Pt-10%Rh thermocouple was used to determine the optical and infrared normal spectral emissivity ($\lambda$ = 0.65 $\mu$m and $\lambda$ = 2 - 2.6 $\mu$m respectively) for the KTFR emitters. The results were:

$$\epsilon_\lambda(\lambda = 0.65\ \mu\text{m}) \approx 0.8 \text{ for } T \approx 1020 - 1090\ \text{K}$$

$$\epsilon_\lambda(\lambda = 2 - 2.6\ \mu\text{m}) \approx 0.3 \text{ for } T \approx 710 - 1090\ \text{K}$$

These spectral-emissivity values are somewhat higher than those of standard oxide cathodes, where a value of $\epsilon_\lambda(\lambda = 0.65\ \mu\text{m}) \approx 0.25 - 0.3$ is normally used. The visual coloration is also somewhat more grayish in appearance due to the higher carbon content remaining from the KTFR binder, a fact that was also confirmed by observing an unusually large carbon peak on these cathodes using Auger-electron spectroscopy. However, a more rapid conversion of KTFR cathodes would provide greater oxidation of residual carbon by the increased $CO_2$ pressure from the alkaline earth carbonate decomposition. This results in a more whitish appearing surface or one having a somewhat lower spectral

*The KTFR cathodes were supplied by B.V. Dore, Electron Emission Systems, Inc., Tucson, AZ. 85713.
†Sylvania C14 powder containing 45% barium carbonate, 51% strontium carbonate, and 4% calcium carbonate with a particular size of 1.2 ± 0.3 $\mu$m, obtained from GTE Sylvania, Emporium, PA. 15834.

UNCLASSIFIED

emissivity.* Consequently, unless $\epsilon_\lambda$ for a specific emitter is known, temperatures determined optically might be in error by ±50 K. For this reason, only thermocouple temperatures were used in these measurements. As a final check, the thermal emf generated in the emitter-thermocouple structure was measured in a separate calibrated oven after the emission experiments and was found to be accurate to within ±10 K.

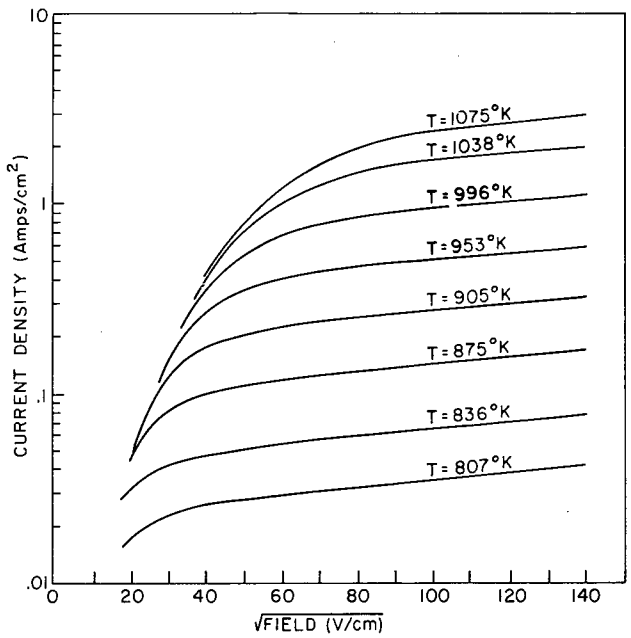


Fig. 1—Pulsed Schottky plots on a 3-mm-diameter planar emitter. The pulse width was 200 μs, with a pulse repetition rate of 60 pps.

Figure 1 is a sample set of pulsed Schottky plots taken on one 3-mm-diameter planar emitter. The pulse width was 200 μs, with a pulse repetition rate of 60 pps. No significant decay in emission was observed during the pulse. The Schottky slopes fell within 10 - 15% of the theoretical value of 1.91/T, as determined by

$$\log_{10} j = \log_{10} j_0 + \frac{1.91}{T}\sqrt{F}, \tag{1}$$

where j and $j_0$ are the current density (A/cm$^2$) at field values of F (V/cm) and zero respectively and T is the temperature in degrees Kelvin. The Schottky curves are quite straight beyond the space-charge region, indicating a relatively uniform or patch-free emitter. Figure 2 is a plot of the effective work function $\phi_E(T)$ defined by

$$j_0(T) = 120T^2 10^{-5040\ \phi_E(T)/T}, \tag{2}$$

where $j_0(T)$ is the extrapolated zero-field current density obtained from Schottky data of the type given in Fig. 1 and $\phi_E(T)$ is in volts. Both the pulsed and dc Schottky data

*B. V. Dore, private communication.

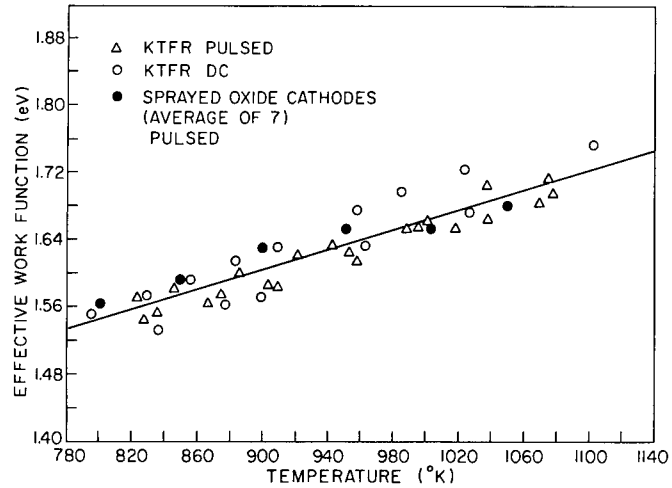


Fig. 2—Effective work function $\phi_E(T)$ vs temperature T for both pulsed and dc measurements of KTFR cathodes. The solid points are the average $\phi_E(T)$ for seven standard sprayed oxide-coated cathodes.

measurements from which the data in Fig. 2 were derived were taken dynamically using logarithmic and square-root amplifiers. Figure 2 shows that the pulsed and dc effective work functions are approximately equal and that the temperature dependence of $\phi_E$ is approximately $6.3 \times 10^{-4}$ eV/K. Scatter in $\phi_E$, which is ±50 mV, is the result of normal variations in emitter preparation, composition, tube processing, etc. For comparison purposes, Fig. 2 also shows the average pulsed $\phi_E(T)$ of seven sprayed oxide-coated cathodes. Scatter in the sprayed cathodes was comparable to the KTFR emitters. Consequently, it is seen that even though the residual carbon content might be higher, the oxide cathodes using KTFR as the binder are comparable in emission to standard sprayed oxide-coated cathodes.

## MEASUREMENTS USING THE SCANNING LOW-ENERGY ELECTRON PROBE AND AN AUGER SPECTROMETER

Surface potential and chemical studies were also made on pentode devices which were obtained from Electron Emission Systems Corporation of Tucson, Arizona. The pentodes were fabricated by sputtering approximately 2000 Å of tungsten onto a sapphire substrate and photolithographically delineating all electrodes. The cathode was prepared from the KTFR oxide cathode mixture described in the previous section. The cathode area was also delineated on the tungsten-substrate electrode by photolithographic techniques. Figure 3 is an optical photomicrograph of one pentode device taken with both reflected and transmitted light. The sequence of electrode widths and spacings (in mils) starting from the far right (the grid which surrounds the cathode) is: 2, 2, 4, 2, 4, 2, 2, 1, 2, 2, 2, 2, 2. The length of the cathode is 0.100 in. The white dots are holes in the sputtered tungsten heater film which was deposited on the rear surface of the sapphire chip. The device was inserted into the combined SLEEP (6) and Auger-spectrometer system shown in Fig. 4.

The system was exhausted to a base pressure of approximately $10^{-10}$ torr. The spectrum of the background gas, measured with the quadrupole mass spectrometer, is shown in Fig. 5. It is seen that ambient gases consist of typical residual $H_2$, $H_e$, $CH_3$

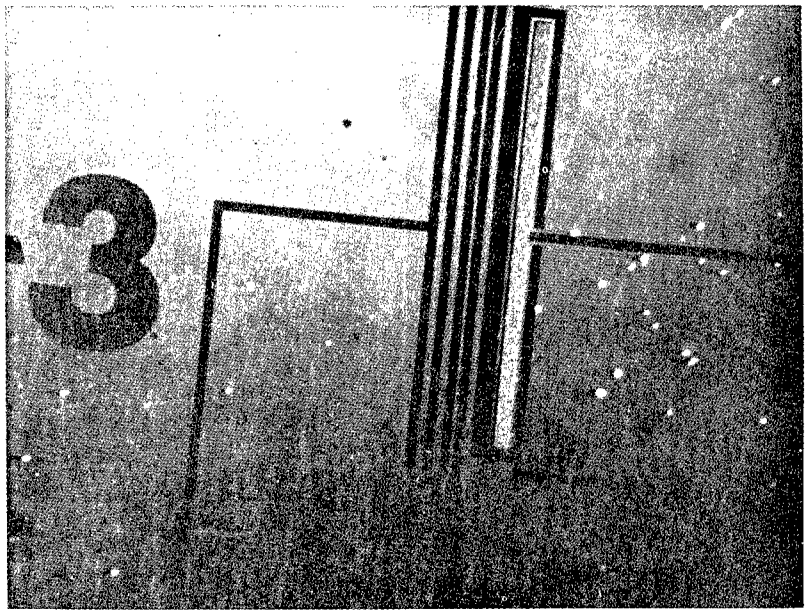

Fig. 3—Photomicrograph of a vacuum-integrated-circuit pentode device on a sapphire substrate. On the right is seen the cathode surrounded by the control grid. To the left of the control grid are the screen grid, suppressor grid, anode electrode, and repeller grid. The length of the electrodes is approximately 0.100 in., and the sequence of electrode widths and spacings (in mils) starting from the far right is 2, 2, 4, 2, 4, 2, 2, 1, 2, 2, 2, 2, 2.

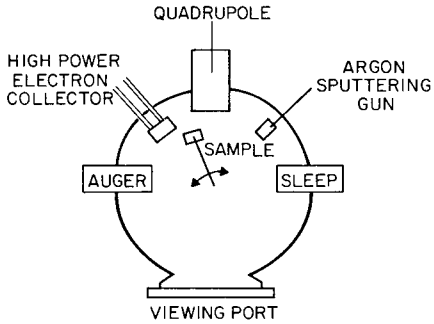


Fig. 4—UHV experimental chamber in which the vacuum integrated-circuit pentode devices were studied.

$CH_4$, HF, CO, $N_2$, $CO_2$ etc. The device was activated by heating at a rate of 30 C/min to 750 C, and then at 15 C/min to the activation temperature of approximately 900 C (brightness). Figure 6 is a SLEEP kinescope photograph of the surface work-function topography of the pentode device. The light areas are regions of low surface potential (work function), and the dark areas are regions of high surface potential. The work function of the cathode was about 2 eV, as measured with both thermionic-emission techniques using Schottky plots, as described in the previous section, as well as with retarding-potential techniques using a $< 114 >$ tungsten single crystal as the reference work function. The gaussian half width in the work-function distribution was measured to be 0.1 eV.

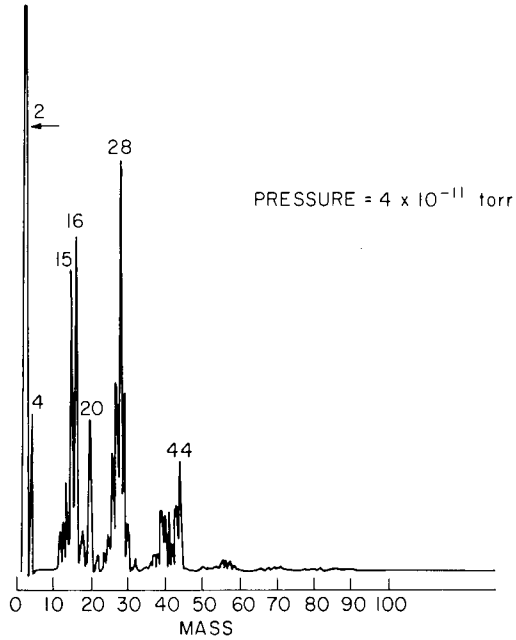


Fig. 5—Spectrum of the background gas in the UHV chamber shown in Fig. 4. Note that the gas load consists of the typical gases $H_2$, $H_e$, $CH_3$, $CH_4$, HF, CO, $N_2$, $CO_2$, etc.

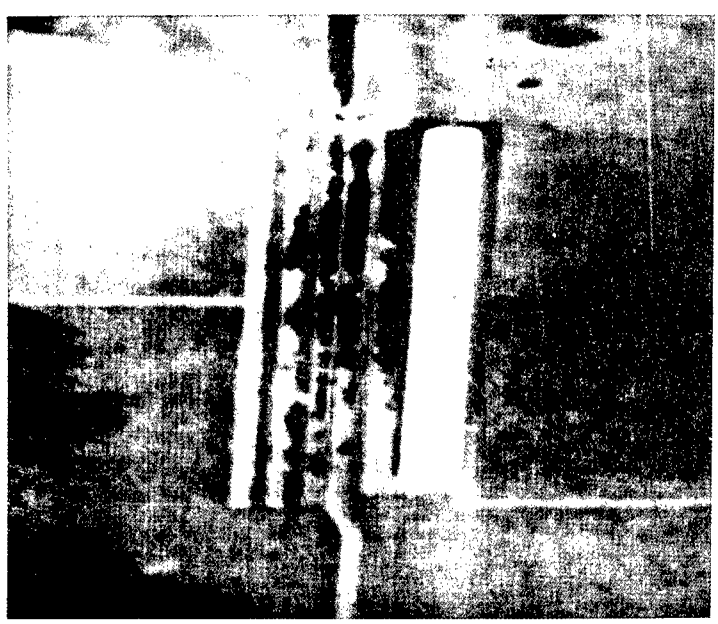

Fig. 6—SLEEP kinescope display of the surface work-function topography of the pentode device. The light areas are regions of low work function, and the dark areas are regions of high work function. The work function of the cathode is about 2 eV.

UNCLASSIFIED

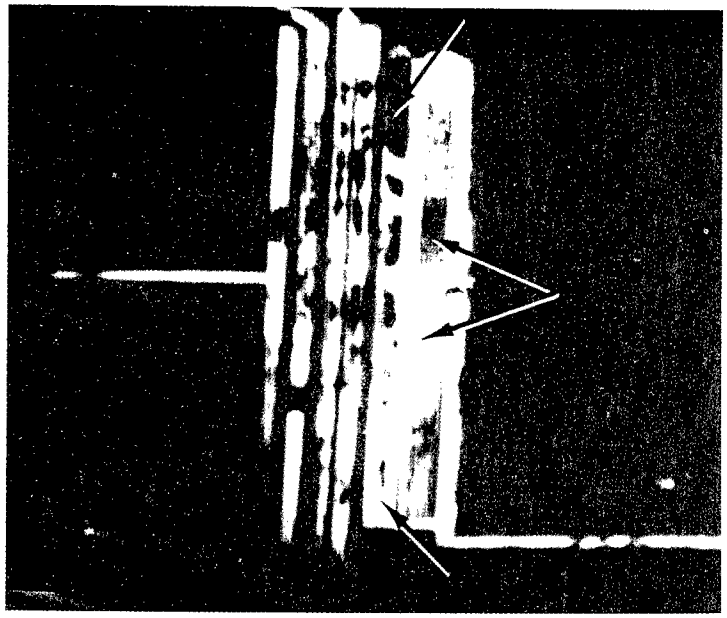

Fig. 7—SLEEP kinescope display of the pentode device after about 250 hr at 700°C. The variation in cathode work function, indicated by the upper and lower central arrows, ranges from approximately 4.25 to 4.00 eV respectively. The variation of surface potential of the control grid which surrounds the cathode, indicated by the top and bottom arrows, ranges from approximately 4.75 to 3.75 eV respectively.

After about 250 hr at 700 C, the emitter work function had degraded and become nonuniform, as is shown in the work-function kinescope picture, Fig. 7. The variation in cathode work function, from 4.25 to 4.00 eV, was obtained from the regions indicated by the upper and lower central arrows respectively in Fig. 7. The surface potential of the grid surrounding the cathode also showed variations ranging from 4.75 to 3.75 eV, which were obtained from the regions indicated by the top and bottom arrows respectively.

Auger-electron spectra of the high- and low-surface-potential regions of the grid structure are shown in Fig. 8. Region A is that of high surface potential (upper arrow in Fig. 7), and region B is that of low surface potential (lower arrow in Fig. 7). It is seen that the lower-surface-potential region is associated with a higher amount of carbon and sulfur on the surface and a smaller amount of tungsten. A possible reason for the lower surface potential of region B is the formation of a tungsten carbide whose work function is lower than that of the more typical oxygen-covered tungsten.

Figure 9 is an Auger spectrum of the emitter surface which shows the barium and oxygen peaks, as well as a strong peak due to the residual carbon remaining from the photoresist binder, in agreement with the spectral emissivity measurements of the previous section. The barium/oxygen peak-height ratio is identical to that obtained from an evaporated film of pure barium oxide used for calibration. Also seen in the Auger spectrum are peaks due to sulfur and small regions of the tungsten substrate.

Figure 10 is an Auger spectrum of the $Al_2O_3$ substrate surface. It shows the typical aluminum peak at 1396 eV and an oxygen peak at 506 eV. The characteristic downward shift of the oxygen peak from ≈512 eV (Fig. 9) is indicative of the restructuring of the

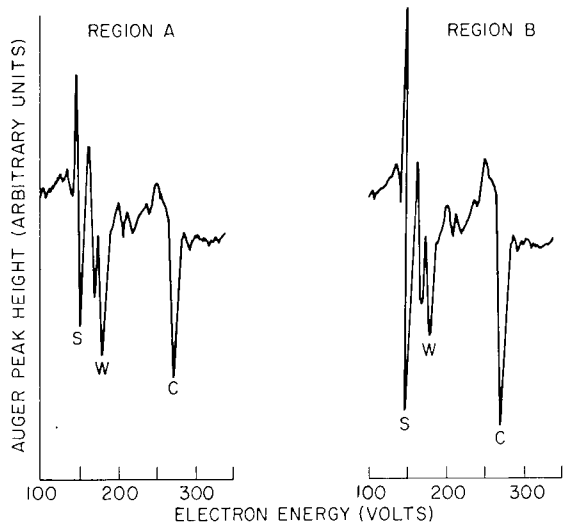


Fig. 8—Auger-electron spectra taken on the pentode device shown in Fig. 7. Region A is that of high surface potential (top arrow in Fig. 7), and region B is that of low surface potential (bottom arrow in Fig. 7).

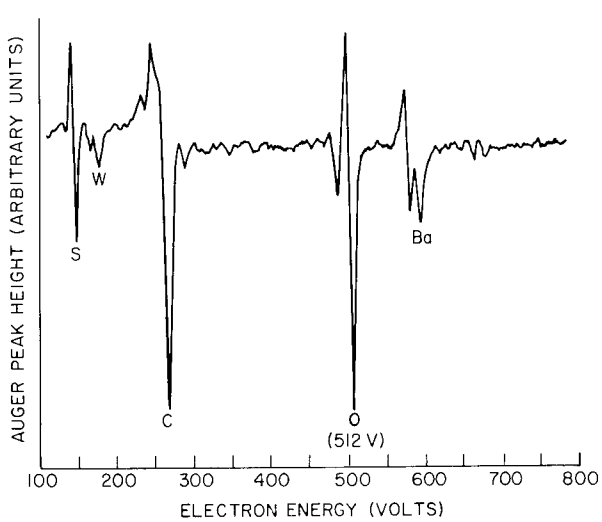


Fig. 9—Auger-electron spectrum of the pentode's cathode made from the KTFR oxide cathode mixture. Also, in addition to the expected oxygen and barium peaks, is the large carbon peak remaining from the photoresist binder.

UNCLASSIFIED

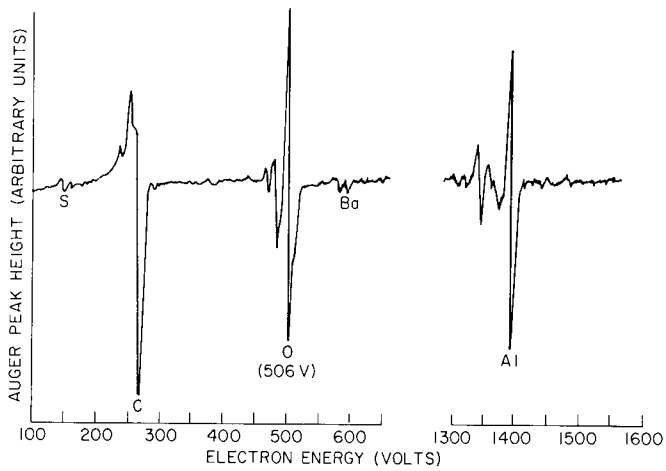


Fig. 10—Auger-electron spectrum of the $Al_2O_3$ substrate surface after extensive heating. Note the 6-eV downward shift of the oxygen peak (from 512 to 506 eV) due to the restructing of the oxygen energy levels in forming the alumina molecule. The shape of the oxygen peak is also altered from that seen in Fig. 9.

oxygen energy levels in forming the alumina molecule. Also evident on the substrate are slight barium and sulfur peaks and a substantial carbon peak.

One of the main areas of interest for vacuum-integrated-circuits is determining the extent of migration of cathode material onto various electrodes and the dielectric-substrate areas which separate them. Figure 11 is an enlarged kinescope photograph of the central portion of the cathode and its surroundings. This scan was taken after extensive heating at about 900 C for about 200 hr to study the effects of migration of low-work-function material (e.g., Ba and 0). The emitter (dark region), had been completely poisoned; regions of tungsten substrate material (originally of high work function) onto which no cathode material was deposited showed a slight migration of low-work-function material (arrows). The dark region between the electrodes has a surface potential of $\approx 6$ eV. Though some barium is on this sapphire surface (Fig. 10), it does not appear to appreciably alter the surface potential. Specifically, the amount of migration along the tungsten lead to the cathode was approximately 60 $\mu$m (right-hand arrow), and the left edge of the tungsten-electrode substrate of the cathode, which was not covered with photoresist emissive material, was now completely covered with low-work-function materials. This stripe is about 15 $\mu$m wide.

In addition to surface-potential measurements on the pentode device using the SLEEP, the device was also studied using incident electrons with energies from 0 to 600 eV. Figure 12 is a kinescope display when the SLEEP apparatus is operated in the scanning-electron-microscope (SEM) mode with an incident electron energy of 600 eV. The secondary-electron topograph shows a definite device defect which connects the anode electrode to the suppressor grid (in the lower left portion of the device). Such a defect could cause partial electrical shorting between electrodes. In this case, however, the electrical degradation between these two electrodes was masked due to the overall low resistance between electrodes discussed in the next paragraph.

Serious charging of the sapphire substrate by electrons incident on it (using the SLEEP electron beam) was observed on the initial cold substrate. The charging effect,

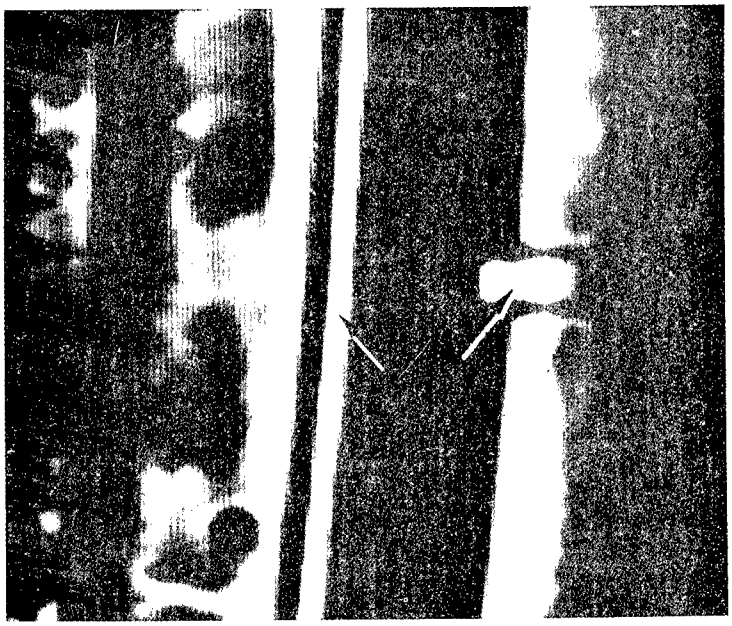

Fig. 11—SLEEP kinescope display of the central portion of the cathode after extensive heating at about 900 C for 200 hr. The cathode is completely poisoned. The right arrow shows that low-work-function material has migrated about 60 $\mu$m down the cathode lead, and the left arrow shows that the 15-$\mu$m-wide portion of the tungsten substrate electrode not originally covered by emissive material is now covered.

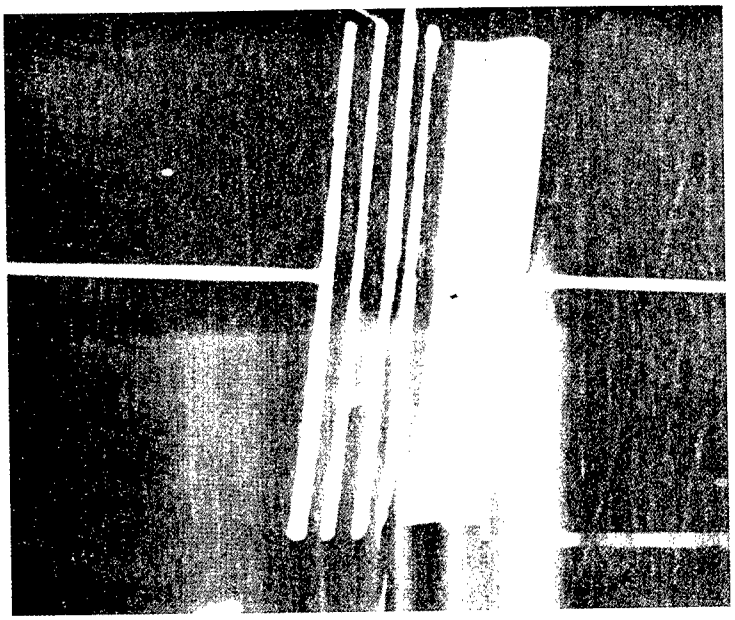

Fig. 12—Secondary-electron kinescope display for incident electrons of 600 eV. A large defect interconnection between the anode and suppressor grid is seen in the lower left portion of the device.

UNCLASSIFIED

however, completely disappeared after heating and activation. This is probably the result of a decrease in the surface resistance of the sapphire substrate after activation of the cathode. In fact, after activation the resistance between grids varied typically from 2000 to 4000 ohms when cold to about 1000 to 2000 ohms when heated to 700 C. These measured resistance values are orders of magnitude less than that which would be expected for a clean $Al_2O_3$ surface. This extremely low resistance, which eliminates the charging effect after activation, is probably caused by the slight barium (or perhaps carbon) layer shown in Fig. 10.

Though the sapphire substrate between grid and cathode has a relatively high work function even after extensive heat treatment, a shading in work function is seen on the grid electrode surrounding the cathode (Fig. 11). The sides adjacent to the cathode have a lower work function than the sides farther away from the cathode. However, this difference in work function is not as large as that caused by the carbon and sulfur variations noted in Figs. 7 and 8.

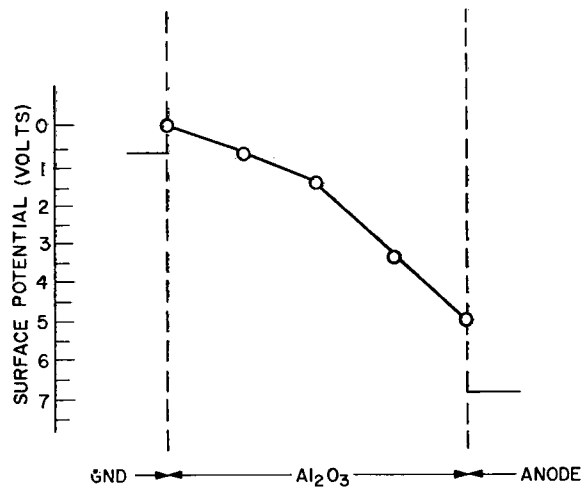


Fig. 13—Variation in surface potential between the repeller and anode leads when a 5-V potential difference is placed between them. The short horizontal lines above "gnd" and "anode" mark the fermi levels of the two leads. The 0 of potential has been arbitrarily placed at the vacuum surface of the repeller lead (gnd).

The variation in surface potential between the repeller and anode leads when a 5-V potential difference is placed between them is shown in Fig. 13. The ordinate is arbitrarily set at 0 V for the surface potential of the sapphire next to the repeller lead. This is about 6 eV above the Fermi level, i.e., the work function of the sapphire is about 6 eV. It is seen that the surface-potential variation in the $Al_2O_3$ is not quite linear, indicating a somewhat higher surface field (and perhaps higher resistivity) near the anode region. The anode-electrode work function for this particular case was $\approx$4 eV (or $\approx$2 eV lower in surface potential than the $Al_2O_3$); the repeller electrode had a work function of $\approx$5 eV (or $\approx$1 eV lower in surface potential than the $Al_2O_3$).

## CONCLUSIONS

- The KTFR-cathode emission is the same as the standard-oxide-coated-cathode emission.

- The spectral emissivity $\epsilon_\lambda$ depends on the cathode activation procedure. Differences in reported work functions (7) for KTFR cathodes might be a result of this uncertainty in $\epsilon_\lambda$.

- The KTFR cathodes have a high residual carbon content.

- The pentode cathode, which was obtained from Electron Emission Systems, Inc., was easily poisoned in the UHV experimental chamber which was used for these studies. (Residual sulfur might have contributed.)

- Surface-potential differences of $\approx$1 eV appeared in various regions of the grid electrodes. These potential variations, which seemed to be correlated with differences in carbon and sulfur, can cause appreciable offset-voltage characteristics for different regions of the device.

- Though very slight barium migration ($<$100 $\mu$m) was observed on the metal substrate, evaporation and vapor transport caused barium from the cathode to appear on leads, electrodes, and substrates. However, in no case did this cause a lowering in the work function approaching that of fully activated cathodes. Consequently, no extraneous emission from these electrodes would be expected.

- No appreciable surface charging was observed, but this was probably due to the lowering of the surface resistance of the $A1_2 0_3$ caused by evaporated barium, carbon, etc. during activation of the cathodes.

In summary, the KTFR emitter is capable of providing the excellent electron emission of oxide-coated cathodes and can be delineated into small areas of any desired shape and size. However, procedures must be found to prevent impurity constituents, which are released during processing as an IC component, from poisoning the cathode, causing low-resistance paths between electrodes and forming significant potential variations on the electrodes themselves.

## REFERENCES

1. D.V. Geppert, B.V. Dore and R.A. Mueller, "Low Temperature Thermionic Emitter," Interim Scientific Report, NASA Contract NAS 12-607, SRI Project PMU-7147, Stanford Research Institute, May 19, 1969.

2. A. Rosengreen, "Investigations of Failure Mechanisms in Integrated Vacuum Circuits," Final Report, NASA contract NAS CR-112108, SRI Project PYU-1257, Stanford Research Institute, Aug. 1972.

3. I.G. Hermann and P.S. Wagner, *The Oxide Coated Cathode*, Chapman and Hall, London, 1951.

4. W.H. Kohl, *Handbook of Materials and Techniques for Vacuum Devices*, Reinhold, New York, 1967.

UNCLASSIFIED

5. G.A. Haas, "Thermionic Electron Sources," in *Methods of Experimental Physics*, Vol. 4, Academic Press, New York, 1967.

6. G.A. Haas and R.E. Thomas, "Electron Beam Scanning Technique for Measuring Surface Work Function Variations," Surface Science 4, 64 (1966).

7. B. Smith, "Thermionic Emission from Oxide-Coated Cathodes at Low Temperatures," ECOM-3585, U.S. Army Electronics Command, Ft. Monmouth, N.J., June 1972.